Published in final edited form as:
*Arch Neurol*. 2012 April ; 69(4): 482–489. doi:10.1001/archneurol.2011.2023.

# Age-Dependent Structural Connectivity Effects in Fragile X Premutation

**Jun Yi Wang, PhD**, **David H. Hessl, PhD**, **Randi J. Hagerman, MD**, **Flora Tassone, PhD**, and **Susan M. Rivera, PhD**
Departments of Psychiatry and Behavioral Sciences (Drs Wang and Hessl), Pediatrics (Dr Hagerman), Biochemistry and Molecular Medicine (Dr Tassone), and Psychology (Dr Rivera), Center for Mind and Brain (Drs Wang and Rivera), and Medical Investigation of Neurodevelopmental Disorders (MIND) Institute (Drs Hessl, Hagerman, Tassone, and Rivera), University of California–Davis, Sacramento

## Abstract

**Objective—**To examine the effects of premutation alleles on major brain fiber tracts in males.

**Design—**Cross-sectional study performed in 2007–2009.

**Setting—**Institutional practice.

**Patients—**Fifteen younger (18–45 years old) carriers, 11 older (>45 years old) unaffected carriers, and 15 older carriers with fragile X–associated tremor/ataxia syndrome, together with 19 younger and 15 older controls matched by age and educational level.

**Main Outcome Measures—**Diffusion tensor imaging was performed on all study participants. Eleven fiber tracts important for motor, social, emotional, and cognitive functions were reconstructed and quantified. Complementary tract-based spatial statistical analyses were performed in core white matter.

**Results—**In the younger carriers, premutation status was associated with a greater age-related connectivity decline in the extreme capsule. Among older carriers, unaffected individuals did not display structural alterations, whereas the affected carriers showed connectivity loss in 5 fiber tracts and exhibited greater age-related connectivity decline in all 11 tracts compared with the controls. In addition, 9 fiber tracts showed significantly higher variability relative to the controls, and symptom severity explained the variability in 6 measurements from the superior cerebellar peduncle, corpus callosum, and cingulum.

**Conclusions—**The findings revealed widespread alterations in structural connectivity associated with fragile X–associated tremor/ataxia syndrome and preserved or subtle changes in structural connectivity in unaffected carriers. Diffusion tensor imaging is sensitive to pathologic changes in the white matter associated with this neurodegenerative disorder.



**Correspondence:** Susan M. Rivera, PhD, Center for Mind and Brain, 202 Cousteau Pl, Ste 250, Davis, CA 95618 (srivera@ucdavis.edu).

**Author Contributions:** *Study concept and design:* Wang and Rivera. *Acquisition of data:* Wang, Hessl, Hagerman, and Tassone. *Analysis and interpretation of data:* Wang, Hessl, Hagerman, and Rivera. *Drafting of the manuscript:* Wang andHessl. *Critical revision of the manuscript for important intellectual content:* Wang, Hessl, Hagerman, Tassone, and Rivera. *Statistical analysis:* Wang. *Obtained funding:* Hessl, Hagerman, and Rivera. *Administrative, technical, and material support:* Hagerman and Rivera. *Study supervision:* Hessl and Rivera.

**Online-Only Material:** The eAppendix, eFigures, and eTable are available at http://mindbrain.ucdavis.edu/people/jyiwang.

Wang et al examine the effects of premutation alleles on major brain fiber tracts in males, who are at risk of developing fragile X-associated tremor/ataxia syndrome and may manifest subtle cognitive, social, and emotional disturbances before clinical involvement.

Male carriers of premutation CGG repeat expansions (55–200 CGG repeats) of the *FMR1* gene are at risk for developing the late-onset neurodegenerative disorder fragile X–associated tremor/ataxia syndrome (FXTAS).[1] The principal features of FXTAS are progressive intention tremor and ataxia, which typically occur after 50 years of age, primarily in males but also (less frequently) in females.[2] Other features include parkinsonism, peripheral neuropathy, autonomic dysfunction, and progressive cognitive decline, including dementia and psychiatric disorders.[3,4] Pathologic manifestations of FXTAS are patchy loss of axons, myelin, and astroglial cells throughout the brain and spongiosis in the middle cerebellar peduncle (MCP).[5,6] In addition to the problems among the older adults, some young premutation carriers display problems in emotional, social,[7–9] and cognitive processing.[10,11]

White matter integrity in male carriers older than 40 years has recently been studied using a tract-of-interest approach[12] to diffusion tensor imaging (DTI).[13,14] Reduced fiber directionality was found in the MCP and superior cerebellar peduncle (SCP), cerebral peduncle, fornix, and stria terminalis in carriers affected by FXTAS. In carriers without FXTAS, only the MCP and cerebral peduncle showed elevated diffusivity. The present study was intended to provide a comprehensive assessment of structural connectivity in male premutation carriers across the adult lifespan. We investigated whether 11 fiber tracts that were reconstructed using DTI tractography[15,16] showed abnormal aging in carriers in a cross-sectional design. To complement the structural connectivity analysis that provides the mean values in a fiber tract, a voxel-based analysis was conducted to search for localized changes.

## METHODS

### RESEARCH PARTICIPANTS

We recruited 75 research participants primarily through their family relationships with children affected by fragile X syndrome, and controls were unaffected family members or were recruited from the local community. We identified premutation alleles using *FMR1* DNA testing[17–19] and assessed symptoms and stage of FXTAS using detailed neurologic examination.[3,20] To detect early signs of FXTAS, we analyzed the younger and older participants separately using an age of 45 years as the cutoff to ensure that the carriers in the younger group were mostly free of FXTAS symptoms. Fifteen younger premutation carriers and 19 younger controls formed 2 younger groups. Fifteen premutation carriers with FXTAS, 11 older carriers without FXTAS, and 15 older controls formed 3 older groups (Table 1). Within both the younger and older groups, participants were matched for age and years of education. For the FXTAS group, FXTAS stage ranged from 2 to 4 (minor to severe tremor and/or balance problems). The appearance of white matter lesions on T2 and fluid-attenuated inversion recovery (FLAIR) images was examined by one of us (R.J.H.). Most carriers (11–14) with FXTAS had lesions in the MCP, insula, frontal lobes, and corpus callosum. Some (6–8) had lesions in the temporal lobe. In contrast, although many older carriers without FXTAS had lesions visible in the insula, frontal lobes, and temporal lobes (4–7), only a few (1–2) had lesions in the MCP and corpus callosum.

### STANDARD PROTOCOL APPROVALS, REGISTRATIONS, AND PATIENT CONSENTS

All participants signed informed consent forms according to the institutional review boards at the University of California–Davis Medical Center.

## NEUROIMAGE ACQUISITION

Neuroimaging was performed on a Trio 3T magnetic resonance imaging scanner with an 8-channel head coil (Siemens Medical Solutions). Diffusion tensor images with 30 gradient directions were obtained using a single-shot diffusion-weighted EPI sequence in 72 axial sections of 1.9-mm thickness (no gap) with a 243-mm field of vision and a 128 × 128 matrix. The diffusion sensitizing gradients were applied at a *b*-value of 700 s/mm$^2$. Five additional images with minimum diffusion weighting were also obtained.

## IMAGE PROCESSING

We used the software package FSL (www.fmrib.ox.ac.uk/fsl/, University of Oxford) for correcting eddy current and motion in DTI and skull-stripping[21] and conducted DTI tractography using DTI Studio (cmrm.med.jhmi.edu; Johns Hopkins Medical Institute). Fiber tracking adopted a multiple regions-ofinterest (ROIs) approach for achieving higher interrater reliability.[15] We set the fractional anisotropy (FA) threshold to 0.18 and the angle threshold to 70° for fiber tracking to ensure the successful reconstruction of the uncinate fasciculus, a small curved fiber tract. We determined ROI placement based on anatomical location and functional division of the fiber tracts[22–26] and by referencing published methods where available.[27–30]

We reconstructed 11 fiber tracts from 4 categories: (1) motor fiber tracts—cerebral peduncular fibers and cerebellar peduncles; (2) limbic tracts—extreme capsule fibers, cingulum, fornix, and angular bundle; (3) association fibers—arcuate fasciculus, uncinate fasciculus, inferior longitudinal fasciculus, and inferior fronto-occipital fasciculus; and (4) callosal fibers— corpus callosum (Figure 1). Only the fornix body was reconstructed because the body provides measurements with high interrater and test-retest reliability compared with the crus.[31] The arcuate fasciculus was tracked separately into anterior, posterior, and direct fiber regions.[30] It was possible to reconstruct the left direct arcuate (for which there were no missing data) and the right anterior arcuate (for which data were missing from 1 participant); the remaining 4 regions, however, could only be reconstructed from some of the participants (63–69 of 75) because of the high individual variability.[32] For this reason, these 4 fiber regions were replaced by left and right “arcuate complex,” a combination of the 3 fiber regions at each hemisphere. See the eAppendix (available at http://mindbrain.ucdavis.edu/people/jyiwang) for detailed fiber tracking methods.

A total of 38 fiber regions were reconstructed and quantified using FA for fiber directionality, mean diffusivity (MD) for packing density, mean length, and tract volume. To normalize the tract volume, total cranial volume was estimated from the T1-weightedMPRAGEimages using the SIENAX function[33] from FSL. For measurements from each fiber region, interrater reliabilities were tested by 2 raters and were above 0.9. Fiber tracking was performed with the rater masked to the status of the participants.

Because DTI tractography provides mean measurements over large areas, we also applied a voxel-based analysis, using tract-based spatial statistics (TBSS), to detect localized changes. The TBSS program possesses the advantage of assessing FA- and MD-related fiber integrity changes in core white matter, thereby being less affected by partial volume effects associated with inclusion of the gray matter and cerebrospinal fluid and inaccuracies from the normalization procedure.[34] The FA threshold for generating skeleton mask was 0.2.

## STATISTICAL ANALYSIS

For tractography and voxel-based analyses, group differences and group × age interactions in DTI measurements were assessed separately in the younger and older groups. Linear regression was used with age and group as independent variables and individual DTI

measurements as dependent variables. An age × group interaction was included only when it was significant ($P < .05$). The Matlab function regstats was used for predicting individual tractography measurements (The Mathworks Inc). To correct for family-wise errors, we applied a 5% false discovery rate (FDR)[35] implemented in the Matlab FDR function to the combined results across all DTI outcomes and regions. The same procedures were implemented for examining the effect of T2 and FLAIR lesions on tractography measurements. We divided the older premutation carriers into groups with and without T2 and FLAIR lesions in the MCP, insula, temporal lobes, and corpus callosum and performed group comparisons of fiber tracts from these areas. Age was used as a covariate when the 2 groups differed significantly in age. For performing voxel-based comparisons of FA and MD using TBSS, the randomize tool with threshold-free cluster enhancement was used.

## RESULTS

Thirty-two of 38 fiber regions were reconstructed successfully for all 75 participants. Fiber regions from the cerebral peduncle, inferior cerebellar peduncle, extreme capsule, and arcuate fasciculus were missing from 1 to 5 participants. All 5 groups were involved except the younger control group. The missing data points were excluded from the analysis.

eFigure 1 (available at http://mindbrain.ucdavis.edu/people/jyiwang) plots the group means and standard deviation of representative tractography measurements. Although the older asymptomatic carriers showed similar variability in tractography measurements to the controls, the carriers with FXTAS exhibited substantially high variability in many measurements. Consequently, the $F$ test was conducted to identify tractography measurements with significantly higher variability in FXTAS carriers compared with the controls. Thirty of 152 measurements showed significantly higher variability after performing the FDR ($F_{14,14} = 3.8–101.7$, $P < .001–.008$). These measurements came from all fiber tracts except 2 limbic fiber tracts, the fornix body and angular bundle. Most of them (22 of 30) were MD measurements (Table 2).

To investigate whether the higher variability of tractography data in the carriers with FXTAS was due to progression of FXTAS, post hoc regression analyses were performed to predict FXTAS stage using individual tractography measurements showing high variability. Six measurements demonstrated significant correlation with FXTAS stage at an FDR level of 0.05 in the premutation group after age adjustment ($|t| = 3.1–4.2$, $P <.001–.005$). These were the MD of the SCP and the genu, anterior body, and posterior body of the corpus callosum, which showed positive correlation, and tract volume of the left cingulum and mean length of the corpus callosum splenium, which showed negative correlation.

The regression analyses of both the younger and older groups revealed that 41 of 1286 tractography measurements (3.2%) survived an FDR threshold of 0.05 ($P < .002$), showing the age effect, group effect, or age × group interaction. Lower FA, mean length, and tract volume and higher MD were designated as reduced structural connectivity. In the younger groups, the asymptomatic carriers had higher tract volume of one limbic tract (right angular bundle, $t = 3.49$, $P = .001$) and greater age-related decline ($t = −3.56$, $P = .001$) in the FA of another limbic tract relative to the controls (right posterior lateral projections of extreme capsule, Figure 2A and B). In the older groups, although no comparisons survived an FDR of 0.05 between the asymptomatic carriers and controls, when comparing the affected carriers with the controls 12 measurements showed a significant group effect and 6 exhibited a significant group × age interaction (multiple linear regression; $|t| = 3.48–5.73$, $P < .001–.002$). Carriers with FXTAS showed reduced structural connectivity relative to the controls in all 4 fiber tract categories (motor, limbic, association, and callosal fiber tracts) and greater age-related decline in structural connectivity in fiber tracts from limbic, association, and

callosal fiber tracts. In contrast, 1 motor tract, the parietal projections of cerebral peduncle, showed increased FA in FXTAS compared with the controls (Table 3). In the analyses of FXTAS carriers vs the asymptomatic carriers, 9 tractography measurements demonstrated significant group or group × age effects (multiple linear regression; $|t| = 3.62–7.23$, $P < .001–.002$). The FXTAS carriers showed reduced structural connectivity relative to the controls in all 4 fiber tract categories and displayed greater age-related decline in structural connectivity in fiber tracts from 3 categories—limbic, association, and callosal fiber tracts. Figure 2C and D illustrates the representative main effect of group and group × age interaction. Because the *P* value corresponding to an FDR of 0.05 was so low (.002), the results obtained from using an FDR level of 0.1 (corresponding to a *P* value of .01) are also provided in Table 3.

The TBSS program did not detect any group effect or group × age interaction when comparing younger or older asymptomatic carriers with the corresponding control group. When comparing the FXTAS carriers with the controls, TBSS detected lower FA in one association fiber tract (inferior longitudinal fasciculus) and higher MD and lower FA in all corpus callosum regions in the FXTAS carriers. The age and group interaction affected all 11 fiber tracts in the 4 categories, showing greater age-related elevation in MD in the FXTAS carriers compared with that of the controls. Three fiber tracts—the cingulum, inferior fronto-occipital fasciculus, and corpus callosum— also exhibited greater age-related decline in FA in the FXTAS carriers (Table 3 and Figure 2E-H). When the FXTAS carriers were compared with the asymptomatic carriers, only the corpus callosum showed lower FA and higher MD in the FXTAS carriers. The greater age-related MD elevation and FA decline in the FXTAS compared with the asymptomatic carriers affected all 11 fiber tracts except the cerebellar peduncles for MD and affected only the corpus callosum splenium for FA (Table 3).

We also examined how the occurrence of macroscopic T2 and FLAIR lesions affected tractography by superimposing fiber tracts on images without diffusion weighting ($b = 0$ s/mm$^2$). Although no fibers were observed in areas with bright lesions, DTI fibers penetrated areas with less bright lesions. The comparisons of the groups with and without lesions revealed that only the groups with lesions in the MCP and corpus callosum exhibited significantly reduced structural connectivity relative to the groups without lesions at an FDR level of 0.05 (eTable; available at http://mindbrain.ucdavis.edu/people/jyiwang).

## COMMENT

To our knowledge, the current study has provided the first DTI tractography analysis to assess structural connectivity in male fragile X premutation carriers (Figure 1). Tractography with DTI has the advantages of examining structural connectivity more directly than TBSS- and ROI-based analyses. The anatomical locations of fiber tracts are determined by performing tractography in which fibers connecting predefined areas are visualized. In contrast, the anatomical locations in voxel- and ROI-based analyses are determined by looking up the brain atlas. In areas where more than 1 fiber tract exists and that have similar fiber orientations, fiber tracts cannot be distinguished from one another by simply looking at the DTI maps. In addition, DTI tractography provides tract-based measurements that are averaged across the voxels containing the fiber tract and thus may not be sensitive to localized changes. Therefore, we added TBSS analysis for the detection of localized changes. The analyses were conducted in both carriers younger than 45 years who did not have the clinical symptoms of FXTAS and older carriers with and without FXTAS. Structural connectivity changes were detected not only in the carriers affected by FXTAS but also in the younger, asymptomatic carriers. The premutation carriers tended to show higher MD and lower FA, mean length, and fiber volume compared with the controls, as

well as greater age-related elevation in MD and greater age-related decline in the remaining 3 fiber variables. These patterns of change are consistent with our common understanding of the effect of weaker structural connectivity or more rapid aging on DTI measurements.

In the younger carriers, the FA of extreme capsule (right posterior lateral projections) showed significantly accelerated age-related decline compared with the controls (Figure 2A). The volume elevation of right angular bundle in the younger carriers (Figure 2B) may be related to the effect of *FMR1* premutation on white matter development and can be further tested in children with fragile X premutation. In the older groups, although the asymptomatic carriers maintained structural connectivity similar to the controls, the structural connectivity in the carriers with FXTAS was substantially different from that of the controls and showed accelerated aging. Both DTI tractography and TBSS detected lower structural connectivity and integrity in carriers with FXTAS relative to the controls in 5 of the 11 fiber tracts from all 4 fiber tracts categories. The carriers with FXTAS also showed greater age-related decline in structural connectivity and integrity in all 11 fiber tracts (Table 3).

The widespread effect of FXTAS on white matter structural connectivity and integrity was in concordance with previous findings of generalized brain atrophy, widespread low gray matter density, and T2 hyperintensity in the MCP and subcortical white matter in the carriers with FXTAS.[36–38] However, we did not replicate previous findings of increased diffusivity in the MCP and cerebral peduncle in the older *asymptomatic* carriers relative to the controls,[12] although the FXTAS carriers showed reduced structural connectivity in the MCP and cerebral peduncle significant at an FDR level of 0.1 ($P$ = .01) and in the SCP significant at an FDR level of 0.05 ($P$ = .002). The subsequent assessment of the effect of T2 and FLAIR lesions on DTI revealed significantly lower structural connectivity in the group with MCP lesions compared with the group without MCP lesions, providing the direct link between MCP lesions and reduced structural connectivity.

Tractography with DTI also showed a pattern of change contradictory to our common understanding of the effect of neurodegeneration on DTI measurements. The FA values of the parietal projections of cerebral peduncle were higher in the carriers with FXTAS compared with the corresponding control group. Although this may at first glance seem counterintuitive, the FA elevation can be explained by the well-known crossing fiber issue in DTI tractography.[39] The parietal projections of the cerebral peduncle overlapped at the centrum semiovale with the corpus callosum, which sustained a significant amount of neurodegeneration in FXTAS. As shown in the histogram of sectionwise FA, the degeneration of the corpus callosum caused the FA of the cerebral peduncle to increase artificially in the carriers with FXTAS at the axial sections where the 2 fiber tracts intersect (eFigure 2A and B, available at http://mindbrain.ucdavis.edu/people/jyiwang).

In addition to the diverging age effect on structural connectivity between the older carriers with and without FXTAS, the variability of structural connectivity increased significantly among the carriers with FXTAS compared with age-matched controls for 30 tractography measurements from 9 of 11 fiber tracts (except 2 limbic tracts). The tractography measurement that showed the most variability was the MD (22 of 30). Regression analyses using age as a nuisance covariate revealed FXTAS stage as a possible explanation for the higher variability in 6 of the tractography measurements from the SCP, corpus callosum, and cingulum. Typically, FXTAS carriers showed abnormally low MD values in these areas at initial stages of FXTAS but elevated MD at the advanced stages, indicating the high sensitivity of tractography measurements to white matter pathologic changes associated with FXTAS.

The current study was limited by using a cross-sectional rather than a longitudinal design to examine aging in male carriers of the premutation, which is a common problem in the aging literature because of the difficulties of following up the participants for a long period. The sample size was also relatively small, especially for the older asymptomatic carriers. The correlation of DTI measurements with molecular data and cognitive functions was unexplored because of the small sample size.

In conclusion, the present study detected subtle white matter structural changes in the young premutation carriers without FXTAS and widespread age-related deterioration in structural connectivity in carriers with FXTAS. The strength of structural connectivity diverged as the carriers aged. Although the unaffected carriers maintained healthy structural connectivity, the affected carriers showed radical structural deterioration. Even within the group of carriers with FXTAS, the variability of structural connectivity increased significantly in 9 fiber tracts compared with age-matched controls, and FXTAS severity explained the variability for measurements from the SCP, corpus callosum, and cingulum. The DTI structural connectivity analyses were sensitive to pathologic changes associated with FXTAS.

## Acknowledgments

**Financial Disclosure:** Dr Wang receives support as a postdoctoral fellow from the National Institutes of Health. Dr Hessl receives grant support from Roche, Novartis, and Seaside Therapeutics for treatment trials in fragile X syndrome and research support from the National Institutes of Health. Dr Hagerman receives grant support from Roche, Novartis, Seaside Therapeutics, Forest, Johnson and Johnson, and Curemark for treatment trials in fragile X or autism and research support from the National Institutes of Health and the National Fragile X Foundation. Dr Tassone receives research support from the National Fragile X Foundation, UC Davis Health System Research Award, and the National Institutes of Health. Dr Rivera receives research support from the National Institutes of Health.

**Funding/Support:** This work was supported by National Institutes of Health grants HD036071, MH078041, MH077554, NS062412, UL1DE019583, RL1AG032119, RL1AG032115, and TL1DA024854.

**Additional Contributions:** We are grateful to the research participants and their families; to Jenny Tram, BS, Jose Fon, BS, and John Shell, BS, for performing fiber tracking; Jim Grigsby, PhD, John Wang, BS, and Patrick Adams, BS, for image and data collection; and Danielle Harvey, PhD, for statistical support.

## REFERENCES

1. Hagerman RJ, Leehey M, Heinrichs W, et al. Intention tremor, parkinsonism, and generalized brain atrophy in male carriers of fragile X. Neurology. 2001; 57(1):127–130. [PubMed: 11445641]
2. Jacquemont S, Hagerman RJ, Leehey MA, et al. Penetrance of the fragile X–associated tremor/ataxia syndrome in a premutation carrier population. JAMA. 2004; 291(4):460–469. [PubMed: 14747503]
3. Jacquemont S, Hagerman RJ, Leehey M, et al. Fragile X premutation tremor/ataxia syndrome: molecular, clinical, and neuroimaging correlates. Am J Hum Genet. 2003; 72(4):869–878. [PubMed: 12638084]
4. Juncos JL, Lazarus JT, Graves-Allen E, et al. New clinical findings in the fragile X–associated tremor ataxia syndrome (FXTAS). Neurogenetics. 2011; 12(2):123–135. [PubMed: 21279400]
5. Greco CM, Berman RF, Martin RM, et al. Neuropathology of fragile X–associated tremor/ataxia syndrome (FXTAS). Brain. 2006; 129(pt 1):243–255. [PubMed: 16332642]
6. Greco CM, Hagerman RJ, Tassone F, et al. Neuronal intranuclear inclusions in a new cerebellar tremor/ataxia syndrome among fragile X carriers. Brain. 2002; 125(pt 8):1760–1771. [PubMed: 12135967]
7. Cornish K, Kogan C, Turk J, et al. The emerging fragile X premutation phenotype: evidence from the domain of social cognition. Brain Cogn. 2005; 57(1):53–60. [PubMed: 15629215]

8. Hessl D, Tassone F, Loesch DZ, et al. Abnormal elevation of *FMR1* mRNA is associated with psychological symptoms in individuals with the fragile X premutation. Am J Med Genet B Neuropsychiatr Genet. 2005; 139B(1):115–121. [PubMed: 16184602]
9. Roberts JE, Bailey DB Jr, Mankowski J, et al. Mood and anxiety disorders in females with the *FMR1* premutation. Am J Med Genet B Neuropsychiatr Genet. 2009; 150B(1):130–139. [PubMed: 18553360]
10. Grigsby J, Brega AG, Engle K, et al. Cognitive profile of fragile X premutation carriers with and without fragile X–associated tremor/ataxia syndrome. Neuropsychology. 2008; 22(1):48–60. [PubMed: 18211155]
11. Cornish KM, Kogan CS, Li L, Turk J, Jacquemont S, Hagerman RJ. Lifespan changes in working memory in fragile X premutation males. Brain Cogn. 2009; 69(3):551–558. [PubMed: 19114290]
12. Hashimoto RI, Srivastava S, Tassone F, Hagerman RJ, Rivera SM. Diffusion tensor imaging in male premutation carriers of the fragile X mental retardation gene. Mov Disord. 2011; 26(7): 1329–1336. [PubMed: 21484870]
13. Basser PJ, Pierpaoli C. Microstructural and physiological features of tissues elucidated by quantitative-diffusion-tensor MRI. J Magn Reson B. 1996; 111(3):209–219. [PubMed: 8661285]
14. Basser PJ, Mattiello J, LeBihan D. Estimation of the effective self-diffusion tensor from the NMR spin echo. J Magn Reson B. 1994; 103(3):247–254. [PubMed: 8019776]
15. Huang H, Zhang J, van Zijl PC, Mori S. Analysis of noise effects on DTI-based tractography using the brute-force and multi-ROI approach. Magn Reson Med. 2004; 52(3):559–565. [PubMed: 15334575]
16. Mori S, Crain BJ, Chacko VP, van Zijl PC. Three-dimensional tracking of axonal projections in the brain by magnetic resonance imaging. Ann Neurol. 1999; 45(2):265–269. [PubMed: 9989633]
17. Tassone F, Pan R, Amiri K, Taylor AK, Hagerman PJ. A rapid polymerase chain reaction–based screening method for identification of all expanded alleles of the fragile X (*FMR1*) gene in newborn and high-risk populations. J Mol Diagn. 2008; 10(1):43–49. [PubMed: 18165273]
18. Fu YH, Kuhl DP, Pizzuti A, et al. Variation of the CGG repeat at the fragile X site results in genetic instability: resolution of the Sherman paradox. Cell. 1991; 67(6):1047–1058. [PubMed: 1760838]
19. Tassone F, Hagerman RJ, Taylor AK, Gane LW, Godfrey TE, Hagerman PJ. Elevated levels of *FMR1* mRNA in carrier males: a new mechanism of involvement in the fragile-X syndrome. Am J Hum Genet. 2000; 66(1):6–15. [PubMed: 10631132]
20. Grigsby J, Brega AG, Jacquemont S, et al. Impairment in the cognitive functioning of men with fragile X–associated tremor/ataxia syndrome (FXTAS). J Neurol Sci. 2006; 248(1–2):227–233. [PubMed: 16780889]
21. Smith SM. Fast robust automated brain extraction. Hum Brain Mapp. 2002; 17(3):143–155. [PubMed: 12391568]
22. Crosby, EC.; Humphrey, T.; Lauer, EW. Correlative Anatomy of the Nervous System. New York, NY: The MacMilan Co; 1962.
23. Nolte, J. The Human Brain: An Introduction to Its Functional Anatomy. 5th ed. St Louis, MO: Mosby; 2002.
24. Augustine JR. Circuitry and functional aspects of the insular lobe in primates including humans. Brain Res Brain Res Rev. 1996; 22(3):229–244. [PubMed: 8957561]
25. Craig AD. Interoception: the sense of the physiological condition of the body. Curr Opin Neurobiol. 2003; 13(4):500–505. [PubMed: 12965300]
26. Craig AD. How do you feel—now? the anterior insula and human awareness. Nat Rev Neurosci. 2009; 10(1):59–70. [PubMed: 19096369]
27. Concha L, Gross DW, Beaulieu C. Diffusion tensor tractography of the limbic system. AJNR Am J Neuroradiol. 2005; 26(9):2267–2274. [PubMed: 16219832]
28. Wakana S, Caprihan A, Panzenboeck MM, et al. Reproducibility of quantitative tractography methods applied to cerebral white matter. Neuroimage. 2007; 36(3):630–644. [PubMed: 17481925]
29. Wakana S, Jiang H, Nagae-Poetscher LM, van Zijl PC, Mori S. Fiber tract–based atlas of human white matter anatomy. Radiology. 2004; 230(1):77–87. [PubMed: 14645885]

30. Catani M, Jones DK, ffytche DH. Perisylvian language networks of the human brain. Ann Neurol. 2005; 57(1):8–16. [PubMed: 15597383]

31. Wang JY, Abdi H, Bakhadirov K, Diaz-Arrastia R, Devous MD Sr. A comprehensive reliability assessment of quantitative diffusion tensor tractography. Neuroimage. [published online ahead of print December 29, 2011].

32. Catani M, Allin MP, Husain M, et al. Symmetries in human brain language pathways correlate with verbal recall. Proc Natl Acad Sci U S A. 2007; 104(43):17163–17168. [PubMed: 17939998]

33. Smith SM, Zhang Y, Jenkinson M, et al. Accurate, robust, and automated longitudinal and cross-sectional brain change analysis. Neuroimage. 2002; 17(1):479–489. [PubMed: 12482100]

34. Smith SM, Jenkinson M, Johansen-Berg H, et al. Tract-based spatial statistics: voxelwise analysis of multi-subject diffusion data. Neuroimage. 2006; 31(4):1487–1505. [PubMed: 16624579]

35. Benjamini Y, Hochberg Y. Controlling the false discovery rate: a practical and powerful approach to multiple testing. J R Stat Soc B. 1995; 57(1):289–300.

36. Brunberg JA, Jacquemont S, Hagerman RJ, et al. Fragile X premutation carriers: characteristic MR imaging findings of adult male patients with progressive cerebellar and cognitive dysfunction. AJNR Am J Neuroradiol. 2002; 23(10):1757–1766. [PubMed: 12427636]

37. Cohen S, Masyn K, Adams J, et al. Molecular and imaging correlates of the fragile X–associated tremor/ataxia syndrome. Neurology. 2006; 67(8):1426–1431. [PubMed: 17060569]

38. Hashimoto R, Javan AK, Tassone F, Hagerman RJ, Rivera SM. A voxel-based morphometry study of grey matter loss in fragile X–associated tremor/ataxia syndrome. Brain. 2011; 134(Pt 3):863–878. [PubMed: 21354978]

39. Mori S, van Zijl PC. Fiber tracking: principles and strategies - a technical review. NMR Biomed. 2002; 15(7–8):468–480. [PubMed: 12489096]

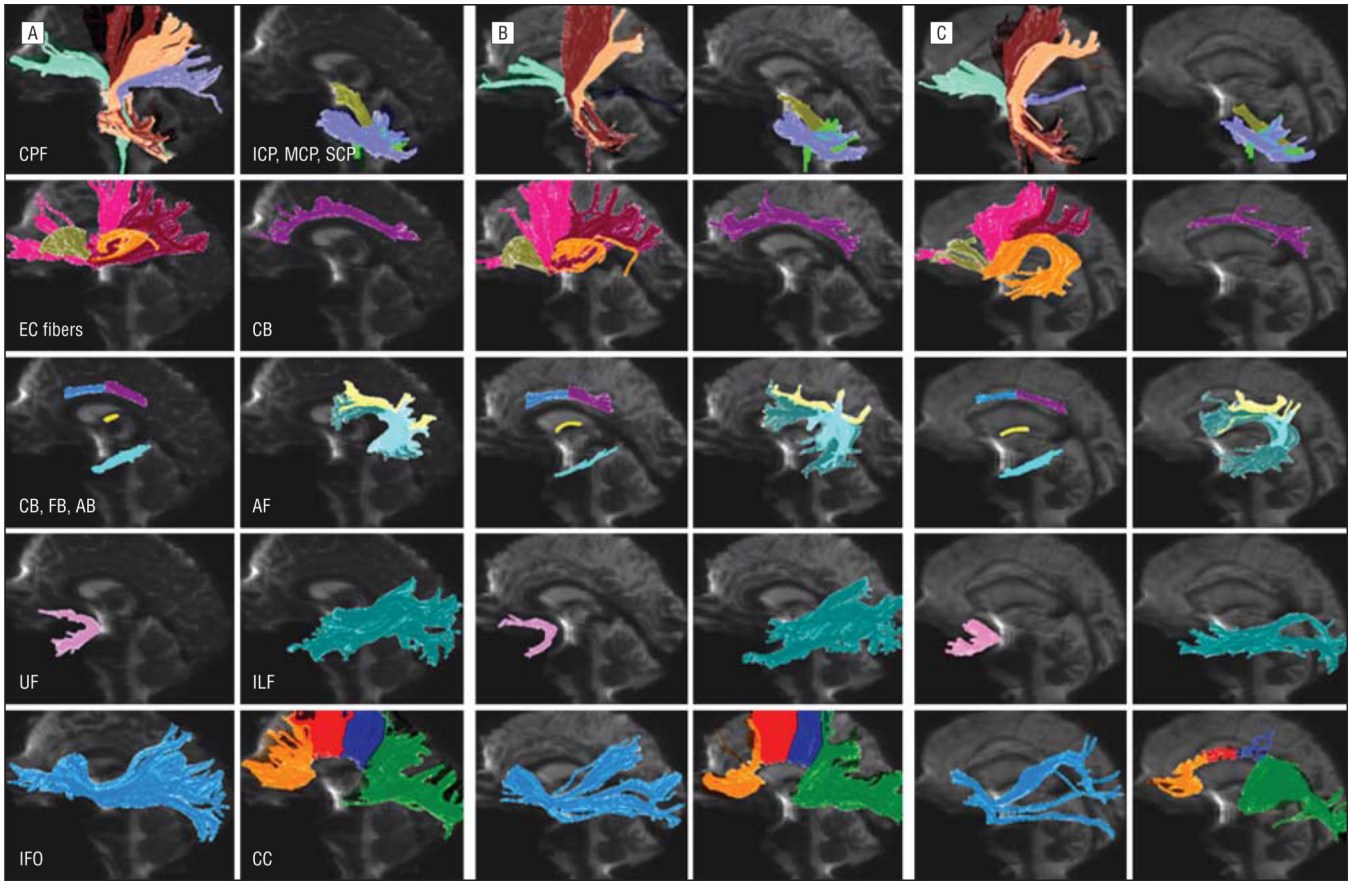


**Figure 1.**

The 11 reconstructed fiber tracts (left-side only) from 3 representative research participants. A, A 53-year-old healthy control; B, a 52-year-old asymptomatic premutation carrier; and C, a 54-year-old premutation carrier with fragile X–associated tremor/ataxia syndrome stage 4. Cerebral peduncular fibers (CPF) project to the anterior frontal lobes (light green), superior frontal lobes (brown), parietal lobes (light orange), and occipital lobes (purple). The inferior cerebellar peduncle (ICP) is shown in green, the middle cerebellar peduncle (MCP) in purple, and the superior cerebellar peduncle (SCP) in dark yellow. The extreme capsule (EC) fibers contain the anterior medial projections (pink), posterior medial projections (dark red), anterior lateral projections (dark yellow), and posterior lateral projections (orange). The cingulate bundle (CB) is shown in dark purple, the anterior CB in blue, the posterior CB in dark purple, the fornix body (FB) in yellow, and the angular bundle (AB) in light blue. The arcuate fasciculus (AF) complex contains the anterior AF (light yellow), posterior AF (aqua), and direct AF (dark teal). The uncinate fasciculus (UF) is shown in lavender, the inferior longitudinal fasciculus (ILF) in teal, and the inferior fronto-occipital fasciculus (IFO) in blue. The corpus callosum (CC) contains 4 fiber regions: genu (orange), anterior body (red), posterior body (navy blue), and splenium (green).

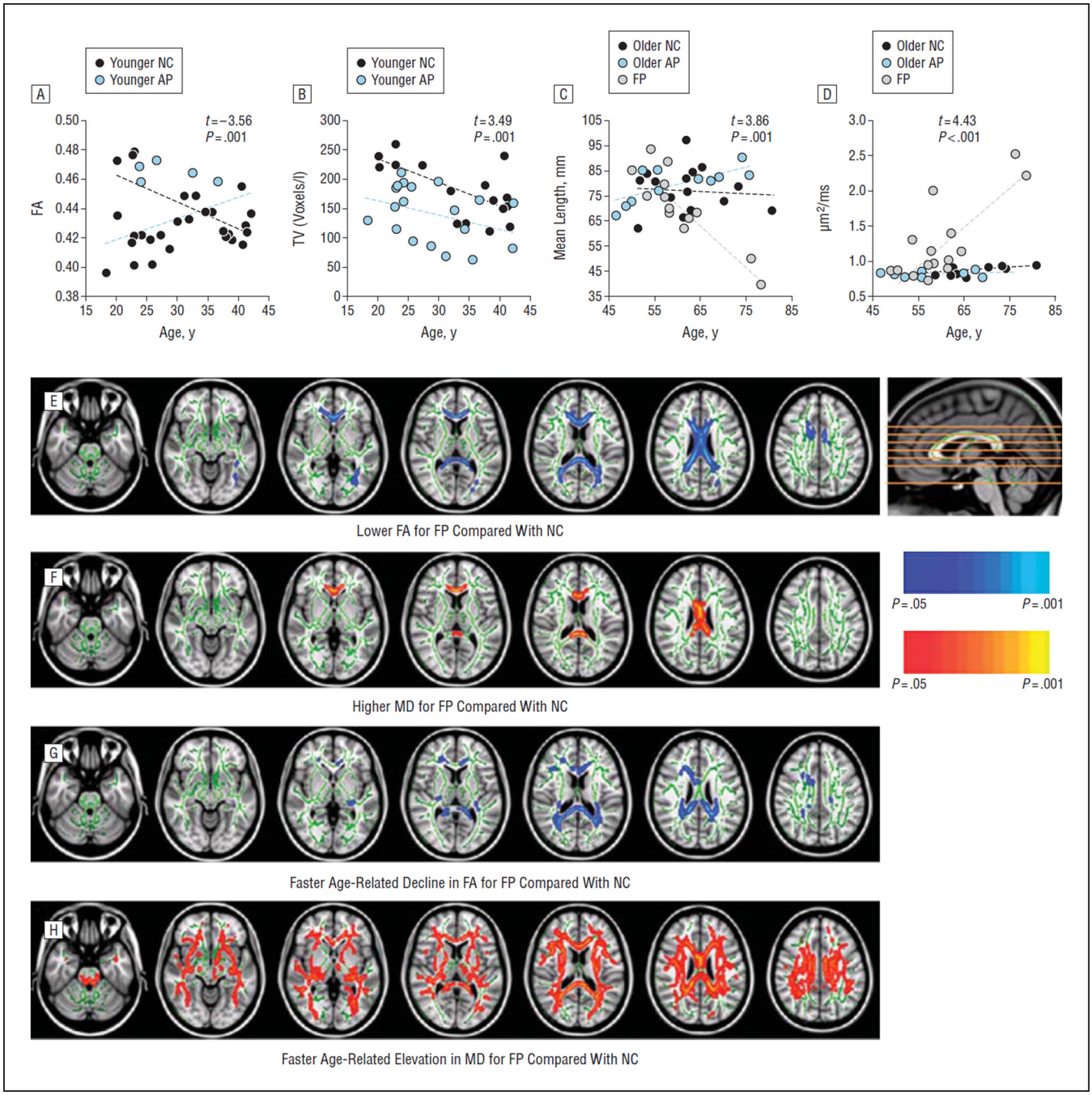


**Figure 2.**

Aging in male carriers of the fragile X premutation. A, The younger asymptomatic carriers showed greater age-related decline in the fractional anisotropy (FA) of right posterior lateral projections (temporal lobe) of the extreme capsule compared with the controls. B, The younger asymptomatic premutation carriers showed higher tract volume (TV) of the right angular bundle relative to the controls. The fragile X–associated tremor/ataxia syndrome (FXTAS) group showed greater age-related decline in the mean length of the left cingulate bundle (C) and significant elevation and greater age-related elevation in the mean diffusivity (MD) of the posterior body of the corpus callosum (D) compared with the control and asymptomatic groups. Tract-based spatial statistics detected white matter areas with

significantly lower FA (E) and higher MD in carriers with FXTAS (F) compared with the controls. Tract-based spatial statistics detected white matter areas with greater age-related decline in FA (G) and greater age-related elevation in MD in carriers with FXTAS (E) compared with the controls. AP indicates asymptomatic premutation carriers; FP, premutation carriers with FXTAS; and NC, normal controls.

**Table 1**

Characteristics of the 75 Research Participants

| | Mean (SD) [Range] | | | | |
|---|---|---|---|---|---|
| | Younger Groups | | Older Groups | | |
| **Characteristic** | **Carriers (n = 15)** | **Controls (n = 19)** | **FXTAS Positive (n = 15)** | **FXTAS Negative (n = 11)** | **Controls (n = 15)** |
| Age, y | 32.9 (8.1) [20–42] | 28.8 (6.9) [18–42] | 60.7 (7.7) [50–79] | 60.1 (10.6) [47–76] | 62.3 (8.1) [52–81] |
| Educational level, y | 15.7 (3.2) [8–21] | 14.8 (3.9) [5–20] | 14.1 (1.9) [12–18] | 15.8 (3.0) [12–20] | 15.0 (3.7) [6–20] |
| FXTAS stage | | | 3.1 (0.7) [2–4] | 0.4 (0.5) [0–1] | |
| *FMR1* CGG length | 95.0 (28.9) [55–157] | 28.3 (3.3) [19–31] | 102.2 (27.1) [62–154] | 80.5 (17.2) [59–113][a] | 28.2 (5.8) [19–42] |
| *FMR1* mRNA level | 3.1 (1.2) [2.2–6.4] | 1.5 (0.3) [1.0–1.9] | 3.2 (0.9) [2.0–5.6] | 2.5 (0.8) [1.4–4.2] | 1.5 (0.2) [1.0–2.0] |

Abbreviations: FXTAS, fragile X–associated tremor/ataxia syndrome; mRNA, messenger RNA.

[a]Compared with the FXTAS-positive group, $t = -2.3$, $P = .03$.

**Table 2**

Tractography Measurements Showing Significantly High Variability in Carriers With Fragile X–Associated Tremor/Ataxia Syndrome[a]

| Fiber Tract | Fiber Variable | Mean (SD) | | *F* | *P* Value |
|---|---|---|---|---|---|
| | | Older NC | FP | | |
| Motor fiber tracts | | | | | |
| Cerebral peduncle: superior frontal | MD | 0.80 (0.032) | 0.81 (0.063) | 4.22 | .005 |
| Cerebral peduncle: parietal | MD | 0.85 (0.031) | 0.83 (0.067) | 4.53 | .004 |
| Cerebellar peduncle: middle | FA | 0.50 (0.017) | 0.47 (0.043) | 6.46 | <.001 |
| Cerebellar peduncle: middle | MD | 0.74 (0.028) | 0.80 (0.081) | 7.91 | <.001 |
| Cerebellar peduncle: superior | MD | 0.96 (0.042) | 1.04 (0.077) | 3.84 | .008 |
| Limbic fiber tracts | | | | | |
| Extreme capsule: left anterior medial | TV | 810 (174) | 871 (394) | 4.73 | .003 |
| Extreme capsule: left posterior medial | MD | 0.83 (0.032) | 0.79 (0.060) | 4.37 | .005 |
| Extreme capsule: right anterior lateral | MD | 0.89 (0.057) | 0.89 (0.116) | 4.07 | .007 |
| Extreme capsule: left posterior lateral | MD | 0.81 (0.035) | 0.81 (0.065) | 3.98 | .007 |
| Extreme capsule: right posterior lateral | MD | 0.82 (0.044) | 0.81 (0.078) | 4.28 | .005 |
| Cingulum: left | TV | 762 (158) | 598 (343) | 5.18 | .002 |
| Cingulum: left | MD | 0.82 (0.035) | 0.82 (0.093) | 9.19 | <.001 |
| Cingulum: right | FA | 0.49 (0.027) | 0.49 (0.059) | 4.97 | .002 |
| Cingulum: right anterior | MD | 0.78 (0.054) | 0.80 (0.094) | 4.26 | .005 |
| Cingulum: left posterior | TV | 162 (35) | 140 (69) | 4.03 | .007 |
| Cingulum: left posterior | MD | 0.77 (0.041) | 0.78 (0.107) | 6.88 | <.001 |
| Association fiber tracts | | | | | |
| Arcuate: left complex | MD | 0.81 (0.032) | 0.81 (0.078) | 7.88 | <.001 |
| Arcuate: right complex | MD | 0.81 (0.036) | 0.81 (0.072) | 7.76 | <.001 |
| Arcuate: left | MD | 0.80 (0.035) | 0.81 (0.078) | 6.64 | <.001 |
| Uncinate: left | MD | 0.87 (0.037) | 0.85 (0.075) | 4.16 | .006 |
| Uncinate: right | MD | 0.85 (0.034) | 0.82 (0.068) | 4.32 | .005 |
| Inferior longitudinal: left | MD | 0.85 (0.032) | 0.82 (0.067) | 6.16 | <.001 |
| Inferior fronto-occipital: left | MD | 0.88 (0.029) | 0.85 (0.063) | 5.36 | .002 |
| Callosal fiber tracts | | | | | |

| Fiber Tract | Fiber Variable | Mean (SD) | | *F* | *P* Value |
|---|---|---|---|---|---|
| | | Older NC | FP | | |
| Corpus callosum: genu | MD | 0.96 (0.076) | 1.09 (0.190) | 8.06 | <.001 |
| Corpus callosum: anterior body | MD | 0.83 (0.059) | 1.03 (0.328) | 40.3 | <.001 |
| Corpus callosum: posterior body | MD | 0.86 (0.055) | 1.17 (0.443) | 101.7 | <.001 |
| Corpus callosum: splenium | ML | 107 (7.2) | 99 (17.8) | 10.0 | <.001 |
| Corpus callosum: splenium | TV | 5181 (533) | 4547 (1140) | 7.06 | <.001 |
| Corpus callosum: splenium | FA | 0.58 (0.027) | 0.57 (0.054) | 5.75 | .001 |
| Corpus callosum: splenium | MD | 0.91 (0.032) | 0.99 (0.178) | 61.7 | <.001 |

Abbreviations: FA, fractional anisotropy; FP, fragile X–associated tremor/ataxia syndrome premutation carriers; MD, mean diffusivity; ML, mean length; NC, normal controls; TV, tract volume.

[a]Listed are tractography measurements that passed the false discovery rate of 0.05 (*P* <.009).

**Table 3**

Group Effect and Group × Age Interaction on Diffusion Tensor Imaging Measurements in the Older Groups[a]

| | Tractography | | | | TBSS | | | |
|---|---|---|---|---|---|---|---|---|
| | NC vs FP | | AP vs FP | | NC vs FP | | AP vs FP | |
| **Fiber Tracts** | **Group Effect** | **Group × Age** | **Group Effect** | **Group × Age** | **Group Effect** | **Group × Age** | **Group Effect** | **Group × Age** |
| Motor fiber tracts | | | | | | | | |
| Cerebral peduncle | *ML*, **FA**[b] | *MD* | *ML* | | | *MD* | | *MD* |
| Cerebellar peduncle | *TV*[b], MD[b] | | *TV*[b] | | | *MD* | | |
| Limbic fiber tracts | | | | | | | | |
| Extreme capsule | *ML, TV*,[b] **FA** | | *ML* | *MD*[b] | | *MD* | | *MD* |
| Cingulum | *ML, TV, MD* | *ML*,[b] *MD*[b] | *ML*[b] | *ML*,[b] *TV, MD*[b] | | *FA, MD* | | *MD* |
| Fornix | *TV, FA*,[b] *MD* | | *FA* | | | *MD* | | *MD* |
| Angular bundle | **MD** | | | | | *MD* | | *MD* |
| Association fiber tracts | | | | | | | | |
| Arcuate | | *MDv* | | *MD* | | *MD* | | *MD* |
| Uncinate | | *MD* | | | | *MD* | | *MD* |
| Inferior longitudinal | *TV*,[b] **FA** | | *TV*[b] | | *FA* | *MD* | | *MD* |
| Inferior fronto-occipital | *TV* | *MD*[b] | | *MD* | | *FA, MD* | | *MD* |
| Callosal fiber tracts | | | | | | | | |
| Corpus callosum | *ML*,[b] TV,[b] MD[b] | *MD* | *ML*,[b] TV,[b] MD | *MD*[b] | *FA* | *FA, MD* | *FA, MD* | *FA, MD* |

Abbreviations: AP, asymptomatic premutation carriers; FA, fractional anisotropy; FP, fragile X–associated tremor/ataxia syndrome premutation carriers; MD, mean diffusivity; ML, mean length; NC, normal controls; TBSS, tract-based spatial statistics; TV, tract volume.

[a] Listed are the tractography measurements that passed the false discovery rate of 0.1 ($P < .01$). Italicized terms indicate higher MD or lower FA, ML, and TV in carriers with fragile X–associated tremor/ataxia syndrome compared with the controls; bold terms, lower MD or higher FA, ML, and TV in carriers with fragile X–associated tremor/ataxia syndrome compared with the controls.

[b] Significant at a false discovery rate of 0.05 ($P < .002$).